

Lawrence Berkeley National Laboratory

Lawrence Berkeley National Laboratory

Title

Magnetic Field Components in a Sinusoidally Varying Helical Wiggler

Permalink

<https://escholarship.org/uc/item/4rw9x65f>

Author

Caspi, S.

Publication Date

1994-07-27

LBL-35928
SC-MAG-464
UC-414

**Magnetic Field Components in a Sinusoidally
Varying Helical Wiggler**

S. Caspi

July 1994

DISCLAIMER

This document was prepared as an account of work sponsored by the United States Government. While this document is believed to contain correct information, neither the United States Government nor any agency thereof, nor The Regents of the University of California, nor any of their employees, makes any warranty, express or implied, or assumes any legal responsibility for the accuracy, completeness, or usefulness of any information, apparatus, product, or process disclosed, or represents that its use would not infringe privately owned rights. Reference herein to any specific commercial product, process, or service by its trade name, trademark, manufacturer, or otherwise, does not necessarily constitute or imply its endorsement, recommendation, or favoring by the United States Government or any agency thereof, or The Regents of the University of California. The views and opinions of authors expressed herein do not necessarily state or reflect those of the United States Government or any agency thereof, or The Regents of the University of California.

Lawrence Berkeley Laboratory is an equal opportunity employer.

SC-MAG-464
LBL—35928

Magnetic Field Components in a Sinusoidally Varying Helical Wiggler.*

Shlomo Caspi

Lawrence Berkeley Laboratory
University Of California
Berkeley, CA 94720

July 27, 1994

* This was supported by the Director, Office of Energy Research, Office of High Energy and Nuclear Physics, High Energy Physics Division, U. S. Department of Energy, under Contract No. DE-AC03-76SF00098.

Abstract

One may be interested in a pure multipole magnetic field (i.e, proportional to $\sin(n\theta)$ or $\cos(n\theta)$) whose strength varies purely as a Fourier sinusoidal series of the longitudinal coordinate z (say proportional to $\cos \frac{(2m-1)\pi z}{L}$, where L denotes the *half-period* of the wiggler and $m=1,2,3 \dots$). Associated with such a z variation, there necessarily will be present a z component of magnetic field which in the source-free region, in fact, will give rise to both normal and skew transverse fields associated with the functions $A_n(z)$ and $\tilde{A}_n(z)$ as expressed in Reference^{bc}. In this note the field components and expression for the scalar potential both inside and outside a thin pure winding surface are included with additional contributions from a possible high permeable shield. It is also shown that for a pure dipole case of $n=1$ and a pure axial variation of $m=1$ the transverse field can be derived from a simple two dimensional field.

Scalar Potential

We note that in the curl-free divergence-free region near the axis $r=0$ the field components may be expressed as given by $\vec{B} = -\nabla V$ where V is a scalar potential function for which $\nabla^2 V = 0$.

$$\frac{1}{r} \frac{\partial}{\partial r} \left(r \frac{\partial V}{\partial r} \right) + \frac{\partial^2 V}{\partial z^2} - \frac{n^2 V}{r^2} = 0 \quad (1)$$

The general form for the proposed solution as shown in Reference c can be written in the form that includes both "skew" and "non-skew" terms of all integer harmonic of order n (including $n=0$):

$$V = - \left\{ \sum_{n=0} r^n \sum_{k=0} \frac{(-1)^{k+1} n!}{2^{2k} k! (n+k)!} r^{2k} \left[A_n^{(2k)}(z) \sin n\theta - \tilde{A}_n^{(2k)}(z) \cos n\theta \right] \right\} \quad (2)$$

and the magnetic field components derived accordingly as :

$$\begin{aligned} B_r &= -\frac{\partial V}{\partial r} = \sum_n [g_{rn} r^{n-1} \sin n\theta - \tilde{g}_{rn} r^{n-1} \cos n\theta] \\ B_\theta &= -\frac{n}{r} V = \sum_n [g_{\theta n} r^{n-1} \cos n\theta + \tilde{g}_{\theta n} r^{n-1} \sin n\theta] \\ B_z &= -\frac{\partial V}{\partial z} = \sum_n [g_{zn} r^n \sin n\theta - \tilde{g}_{zn} r^n \cos n\theta] \end{aligned} \quad (3)$$

where

$$\begin{aligned} g_{rn} &\equiv \tilde{g}_{rn} \\ g_{\theta n} &\equiv \tilde{g}_{\theta n} \\ g_{zn} &\equiv \tilde{g}_{zn} \end{aligned} \quad (4)$$

are general functions of r and z that include the appropriate "normal" and "skew" terms $A_n(z)$ and $\tilde{A}_n(z)$ (see Appendix B).

^b 3D Field Harmonics — S.Caspi , M.Helm , and L.J. Laslett , SC-MAG-328 , LBL-30313 , March 1991.

^c An Approach To 3D Magnetic Field Calculation Using Numerical and Differential Algebra Methods — S.Caspi , M.Helm , and L.J. Laslett , SC-MAG-395 , LBL-32624 , July 1992.

Inner Field $r < R$

For the region within the windings (R equals the thin winding radius) of a helical wiggler such functions and even derivatives of order $(2k)$ are expressed as

$$\begin{aligned}
 A_n(z) &= \sum_{m=1} B_{n,m} \cos \left[(2m-1) \frac{\pi z}{L} \right] \\
 \tilde{A}_n(z) &= \sum_{m=1} B_{n,m} \sin \left[(2m-1) \frac{\pi z}{L} \right] \\
 A_n^{(2k)}(z) &= \sum_{m=1} (-1)^k \left[\frac{(2m-1)\pi}{L} \right]^{2k} B_{n,m} \cos \left[(2m-1) \frac{\pi z}{L} \right] \\
 \tilde{A}_n^{(2k)}(z) &= \sum_{m=1} (-1)^k \left[\frac{(2m-1)\pi}{L} \right]^{2k} B_{n,m} \sin \left[(2m-1) \frac{\pi z}{L} \right]
 \end{aligned} \tag{5}$$

and with the substitution of the above expressions into the scalar potential V (Equation 2)

$$V(r, \theta, z) = \sum_{n=1} n! \sum_{m=1} B_{n,m} \left[\frac{2L}{(2m-1)\pi} \right]^n \sum_{k=0} \frac{1}{k!(n+k)!} \left[\frac{(2m-1)\pi r}{2L} \right]^{2k+n} \sin \left[n\theta - \frac{(2m-1)\pi z}{L} \right] \tag{6}$$

and with

$$I_n(\omega_m r) = \sum_{k=0} \frac{1}{k!(n+k)!} \left(\frac{\omega_m r}{2} \right)^{2k+n} \tag{7}$$

where I_n denotes the "modified" Bessel function (of the first kind and order n),

$$\omega_m = \frac{(2m-1)\pi}{L} \quad \text{and} \quad G_{n,m} = n! \left(\frac{2}{\omega_m} \right)^n B_{n,m} \tag{8}$$

we express the scalar potential (Equation 6) as

$$V(r, \theta, z) = \sum_{n=1} \sum_{m=1} G_{n,m} I_n(\omega_m r) \sin(n\theta - \omega_m z) \tag{9}$$

where for a dipole sextupole , decapole etc, $n=1,3,5,\dots$, $m=1,2,3,\dots$, and L = half period.

The transverse field components and z directed field thus become

$$\begin{aligned}
 B_r &= -\frac{\partial V}{\partial r} = -\sum_{n=1} \sum_{m=1} G_{n,m} \omega_m I_n'(\omega_m r) \sin(n\theta - \omega_m z) \\
 B_\theta &= -\frac{1}{r} \frac{\partial V}{\partial \theta} = -\sum_{n=1} \sum_{m=1} n G_{n,m} \frac{1}{r} I_n(\omega_m r) \cos(n\theta - \omega_m z) \\
 B_z &= -\frac{\partial V}{\partial z} = \sum_{n=1} \sum_{m=1} G_{n,m} \omega_m I_n(\omega_m r) \cos(n\theta - \omega_m z)
 \end{aligned} \tag{10}$$

with

$$I_n'(\omega_m r) = I_{n-1}(\omega_m r) - \frac{n}{\omega_m r} I_n(\omega_m r) \tag{11}$$

where the prime denotes differentiation of the Bessel function with respect to its argument.

Outer Field $r > R$

For a configuration in which the magnetic field components are produced by means of currents confined to lie on the surface of a circular cylinder (radius R), it can be of interest to evaluate the character of the magnetic field components that must be present in the external region ($r > R$) and to determine the components (J_z and J_θ , at R) of current density for this configuration. The surface currents will give rise to a discontinuity of the components B_z and B_θ at the interface ($r=R$), but the normal (radial) component will pass continuously through this surface and assume the form

$$B_r = - \sum_{n=1} \sum_{m=1} G_{n,m} \omega_m \frac{I'_n(\omega_m R)}{K'_n(\omega_m R)} K'_n(\omega_m r) \sin(n\theta - \omega_m z) \quad (\text{for } r \geq R) \quad (12)$$

Consistent with B_r written immediately above a scalar potential function V for the external region is given by

$$V = \sum_{n=1} \sum_{m=1} G_{n,m} \frac{I'_n(\omega_m R)}{K'_n(\omega_m R)} K_n(\omega_m r) \sin(n\theta - \omega_m z) \quad (\text{for } r \geq R) \quad (13)$$

where the prime denotes differentiation of the Bessel functions with respect to its argument, and

$$K'_n(\omega_m r) = - \left[K_{n-1}(\omega_m r) + \frac{n}{\omega_m r} K_n(\omega_m r) \right] \quad (14)$$

The remaining field components are found to be

$$\begin{aligned} B_\theta &= - \sum_{n=1} \sum_{m=1} n G_{n,m} \frac{I'_n(\omega_m R)}{K'_n(\omega_m R)} \frac{1}{r} K_n(\omega_m r) \cos(n\theta - \omega_m z) \\ B_z &= \sum_{n=1} \sum_{m=1} G_{n,m} \omega_m \frac{I'_n(\omega_m R)}{K'_n(\omega_m R)} K_n(\omega_m r) \cos(n\theta - \omega_m z) \end{aligned} \quad (15)$$

Surface currents at $r=R$

The discontinuity of the field components at the interface $r=R$ now permit evaluation of the corresponding surface currents on this cylindrical surface. We denote the current system at the interface $r=R$ by $\vec{J} = J_z \hat{e}_z + J_\theta \hat{e}_\theta$ (amp/m), and recall the relation $\frac{1}{\mu_0} \oint \vec{B} \cdot d\vec{l} = I$ (or $\frac{1}{\mu_0} (\Delta B) = J$), where $\mu_0 = 4\pi 10^{-7}$ in MKS-A units. Then

$$\begin{aligned} J_z(\theta, z)|_{r=R} &= \frac{1}{\mu_0} [B_\theta^{ext.} - B_\theta^{int.}] \\ &= \frac{1}{\mu_0} \sum_{n=1} \sum_{m=1} n G_{n,m} \frac{I_n(\omega_m R) K'_n(\omega_m R) - I'_n(\omega_m R) K_n(\omega_m R)}{R K'_n(\omega_m R)} \cos(n\theta - \omega_m z) \end{aligned} \quad (16)$$

and through the use of the Wronskian $I_n K'_n - I'_n K_n = -\frac{1}{\omega_m R}$

$$J_z(\theta, z)|_{r=R} = -\frac{1}{\mu_0} \sum_{n=1} \sum_{m=1} n G_{n,m} \frac{1}{\omega_m R^2} \frac{1}{K'_n(\omega_m R)} \cos(n\theta - \omega_m z) \quad (17)$$

and

$$\begin{aligned} J_\theta(\theta, z)|_{r=R} &= \frac{1}{\mu_0} [B_z^{int.} - B_z^{ext.}] \\ &= \frac{1}{\mu_0} \sum_{n=1} \sum_{m=1} G_{n,m} \omega_m \frac{I_n(\omega_m R) K_n'(\omega_m R) - I_n'(\omega_m R) K_n(\omega_m R)}{K_n'(\omega_m R)} \cos(n\theta - \omega_m z) \end{aligned} \quad (18)$$

and again through the use of the Wronskian

$$J_\theta(\theta, z)|_{r=R} = -\frac{1}{\mu_0} \sum_{n=1} \sum_{m=1} G_{n,m} \frac{1}{R} \frac{1}{K_n'(\omega_m R)} \cos(n\theta - \omega_m z) \quad (19)$$

The pair of components satisfy the conservation condition $\nabla \cdot \vec{J} = \frac{\partial J_z}{\partial z} + \frac{1}{R} \frac{\partial J_\theta}{\partial \theta} = 0$ as required.

Contribution of axially-symmetric ferromagnetic shield

We realize that if an axially-symmetric ferromagnetic shield of high permeability is present with a radius $r=a$ ($a > R$), the induced magnetization will contribute supplemental fields ("image fields") that in the region interior to $r=a$ may themselves be derived from a scalar potential ($V_{r < a}^{image}$). The appropriate boundary condition at $r=a$ will be fulfilled if we specify that $V_{r=a}^{image} + V_{r=a}^{direct} = \text{constant}$ or if we conveniently specify that $V_{r=a}^{image} = -V_{r=a}^{direct}$ and specifically

$$V_{r=a}^{image} = - \sum_{n=1} \sum_{m=1} G_{n,m} \frac{I_n'(\omega_m R)}{K_n'(\omega_m R)} K_n(\omega_m a) \sin(n\theta - \omega_m z) \quad (\text{at } r = a) \quad (20)$$

If the iron radius is constant (not a function of z) we can write the scalar potential for $r \leq a$

$$V^{image} = - \sum_{n=1} \sum_{m=1} G_{n,m} \frac{I_n'(\omega_m R) K_n(\omega_m a)}{K_n'(\omega_m R) I_n(\omega_m a)} I_n(\omega_m r) \sin(n\theta - \omega_m z) \quad (\text{at } r \leq a) \quad (21)$$

For the TOTAL magnetic potential function at $r < R < a$, we then have

$$V_{r < R}^{total} = \sum_{n=1} \sum_{m=1} G_{n,m} \left[1 - \frac{I_n'(\omega_m R) K_n(\omega_m a)}{K_n'(\omega_m R) I_n(\omega_m a)} \right] I_n(\omega_m r) \sin(n\theta - \omega_m z) \quad (22)$$

The factor contained within the square brackets is an enhancement factor arising from the inclusion of magnetization developed in the high permeability ferromagnetic shield. For the special 2d case where $L \rightarrow \infty$ or $\omega_m a \ll 1$ this factor becomes approximately

$$\lim_{\omega_m a \rightarrow 0} \left[1 - \frac{I_n'(\omega_m R) K_n(\omega_m a)}{K_n'(\omega_m R) I_n(\omega_m a)} \right] = 1 + \left(\frac{R}{a} \right)^{2n} \quad (23)$$

and the potential

$$V_{r < R}^{total-2D} \approx \sum_{n=1} \sum_{m=1} B_{n,m} \left[1 + \left(\frac{R}{a} \right)^{2n} \right] r^n \sin(n\theta - \omega_m z) \quad (24)$$

as expected for the enhancement of the 2D field. For the above approximation we made use of the following asymptotic relations

$$\begin{aligned}
s &\rightarrow 0 \\
I_n(s) &\sim \frac{1}{n!} \left(\frac{s}{2}\right)^n \\
K_n(s) &\sim \frac{(n-1)!}{2} \left(\frac{s}{2}\right)^{-n} \\
I'_n(s) &\sim \frac{1}{2(n-1)!} \left(\frac{s}{2}\right)^{n-1} \\
K'_n(s) &\sim -\frac{n!}{4} \left(\frac{s}{2}\right)^{-(n+1)}
\end{aligned} \tag{25}$$

The square brackets in Equation (22) is plotted in Fig. 4 Appendix A for $n=1$ and $m=1$.

Helical dipole with simple sinusoidal relation

We shall examine a helical dipole with single terms for both series n and m . The choice $n=1$ indicates a pure dipole with no higher harmonics, and $m=1$ indicates a pure $\pi z/L$ variation with no additional frequencies. We express the field components for $r < R$ and $n=m=1$ as

$$\begin{aligned}
\omega_m = \omega_1 &= \frac{\pi}{L}, & G_{n,m} = G_{1,1} &= \frac{2L}{\pi} B_{1,1} \\
B_r &= -2B_{1,1} I'_1\left(\frac{\pi r}{L}\right) \sin\left(\theta - \frac{\pi z}{L}\right) \\
B_\theta &= -2B_{1,1} \left(\frac{L}{\pi r}\right) I_1\left(\frac{\pi r}{L}\right) \cos\left(\theta - \frac{\pi z}{L}\right) \\
B_z &= 2B_{1,1} I_1\left(\frac{\pi r}{L}\right) \cos\left(\theta - \frac{\pi z}{L}\right)
\end{aligned} \tag{26}$$

and

$$\vec{J}(\theta, z) = -\frac{2B_{1,1}}{\mu_0} \left(\frac{L}{\pi R}\right) \frac{1}{K'_1\left(\frac{\pi R}{L}\right)} \left[\hat{e}_\theta + \frac{L}{\pi R} \hat{e}_z \right] \cos\left(\theta - \frac{\pi z}{L}\right) \tag{27}$$

We note that a linear relationship exists between the following field components

$$\frac{B_z}{B_\theta} = -\frac{\pi r}{L} \tag{28}$$

and note as well that for $\frac{\pi r}{L} < \frac{\pi}{2}$ or $r < \frac{L}{2}$ the field components can be expressed with less than 1% error as

$$\begin{aligned}
B_r &= -B_{1,1} \left[1 + \frac{3}{2} \left(\frac{\pi r}{2L}\right)^2 + \frac{5}{12} \left(\frac{\pi r}{2L}\right)^4 + \frac{7}{144} \left(\frac{\pi r}{2L}\right)^6 + \dots \right] \sin\left(\theta - \frac{\pi z}{L}\right) \\
B_\theta &= -B_{1,1} \left[1 + \frac{1}{2} \left(\frac{\pi r}{2L}\right)^2 + \frac{1}{12} \left(\frac{\pi r}{2L}\right)^4 + \frac{1}{144} \left(\frac{\pi r}{2L}\right)^6 + \dots \right] \cos\left(\theta - \frac{\pi z}{L}\right) \\
B_z &= B_{1,1} \frac{\pi r}{L} \left[1 + \frac{1}{2} \left(\frac{\pi r}{2L}\right)^2 + \frac{1}{12} \left(\frac{\pi r}{2L}\right)^4 + \frac{1}{144} \left(\frac{\pi r}{2L}\right)^6 + \dots \right] \cos\left(\theta - \frac{\pi z}{L}\right)
\end{aligned} \tag{29}$$

The representations above will describe a field that formally is both divergence free and curl free — provided that the summations are not truncated. If, however, we wish to truncate these series expressions,

we at best can only do so in such a way that one, but not both, of these conditions is satisfied. Thus, if we wish to preserve the divergence condition $\nabla \cdot \vec{B} = 0$, we should take care that the sum over the k index in the series for B_z should terminate at a value of k that is less by unity than the termination value for this index in the series for the transverse field components B_r & B_θ .

We shall calculate $B_{1,1}$ and compare it with B_{2d} that is produced by a straight long dipole ($L \rightarrow \infty$) carrying the same total current. In the 2D case where a current density (per unit length) of $J(\theta) = J_0 \cos \theta$ and $J_0 = \frac{I_0}{R}$ will produce a dipole field of $B_{2d} = \frac{\mu_0 J_0}{2}$, the dipole field in terms of the total amp-turn is

$$B_{2d} = \frac{\mu_0 I_0}{2R} \quad (30)$$

We shall evaluate the total amp-turn in the helical wiggler by integrating the azimuthal current density along $\theta=0$ using equation (27) (see Fig. 1 below).

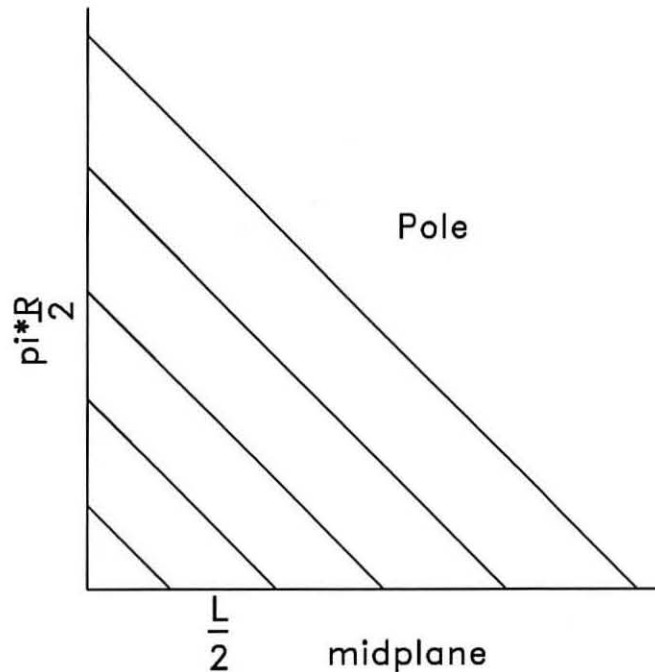
$$I_0 = \int_0^{\frac{\pi}{2}} J_z|_{z=0} R d\theta = \int_0^{\frac{L}{2}} J_\theta|_{\theta=0} dz = -\frac{2B_{1,1}}{\mu_0} \frac{1}{sK_1'(s)} \int_0^{\frac{L}{2}} \cos \frac{\pi z}{L} dz = -\frac{2B_{1,1}R}{\mu_0 s^2 K_1'(s)} \quad (31)$$

By equating the total current in both the 2D dipole and the helical wiggler the ratio of their transverse fields can be reduced to a dimensionless form :

$$\frac{B_{1,1}}{B_{2d}} = s^2 K_1'(s) \quad (32)$$

and note that in the limiting case (using Eq. 25) as $L \rightarrow \infty$

$$\lim_{s \rightarrow 0} \frac{B_{1,1}}{B_{2d}} = 1 \quad (33)$$



as it should be.

The relation between the normalized transverse fields and s (Eq. 32) plotted in Figure 1, reveals a range that surprisingly is grater than 1 where a maximum of 1.0616089 is reached at $s=0.6$. A computational check was made with a cylinder of radius $R=2.0$ cm, surrounded by a current sheet in

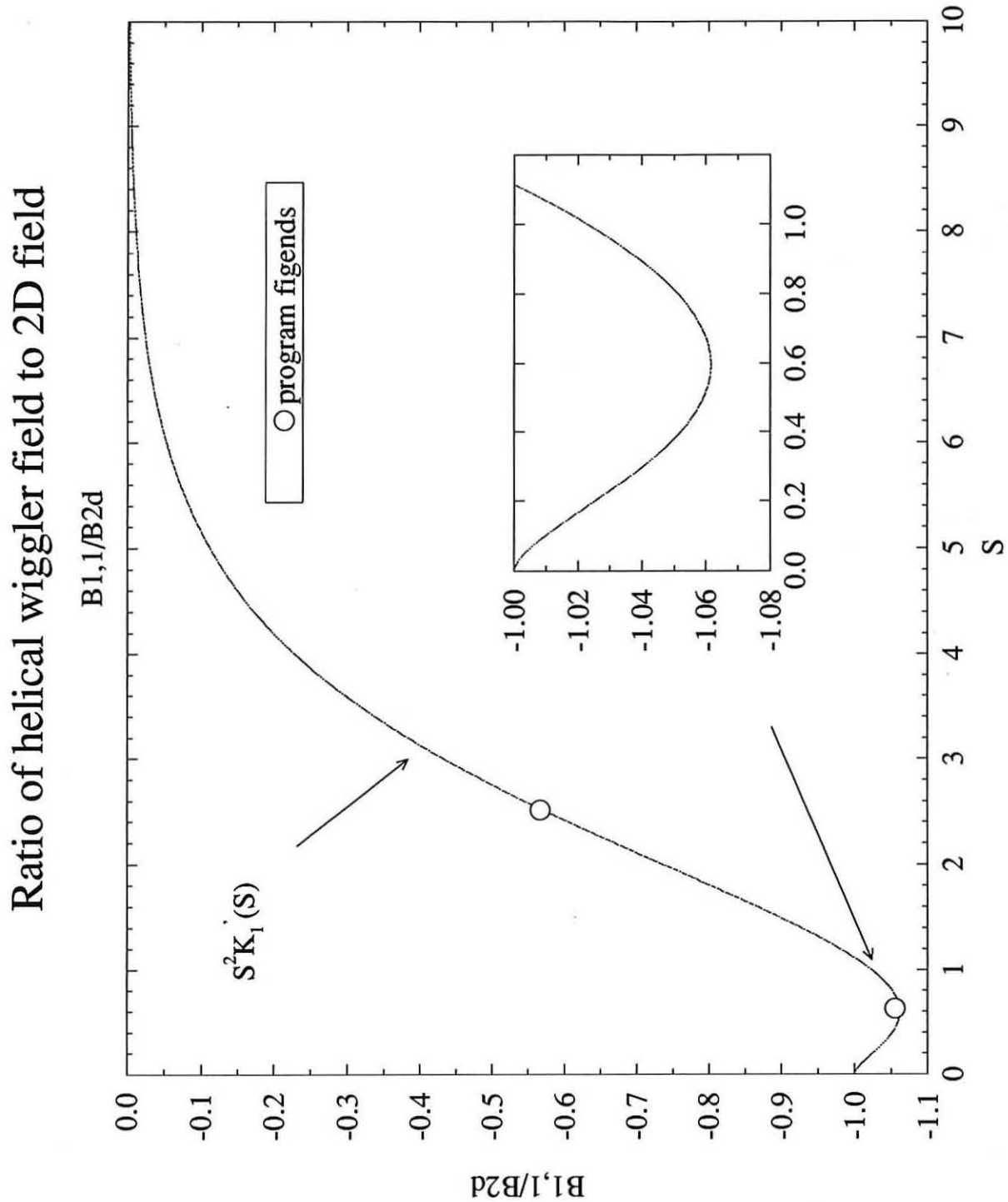


Figure 1 Ratio of wiggler field to 2d dipole field.

a $\cos\theta$ fashion (Figure 2) such that

$$J = \frac{I_0}{R} \cos\theta = 39 \times 10^3 \cos\theta \quad (A/cm) \quad (34)$$

with a dipole field of

$$B_{2d} = \frac{\mu_0 I_0}{2R} = 2.4504 \quad (tesla) \quad (35)$$

(we picked $N=39$ turns, $I=2000$ A and note that $I_0=NI$). A quick check with the 2D program "pkpeak" yields a similar value of $B_{2d}=2.4583$ (tesla). Applying the same current configuration in two examples of a helical wiggler with the same radius R but different periods, such that

$$\begin{aligned} \lambda_1 = 2L = 5 \quad cm \quad , \quad s = \frac{\pi R}{L} = 2.513 \\ \lambda_2 = 2L = 20 \quad cm \quad , \quad s = \frac{\pi R}{L} = 0.6283 \end{aligned} \quad (36)$$

Equation (32) then predicts the following results :

$$\begin{aligned} \frac{B_{1,1}(\lambda_1)}{B_{2d}} = 0.567 \quad or \quad B_{1,1} = 1.3976 \quad (tesla) \\ \frac{B_{1,1}(\lambda_2)}{B_{2d}} = 1.06135 \quad or \quad B_{1,1} = 2.600 \quad (tesla) \end{aligned}$$

With the aid of the 3D program "figends" using a model such as shown in Figure 3, the corresponding values are :

$$\begin{aligned} \frac{B_{1,1}(\lambda_1)}{B_{2d}} = 0.5652 \quad or \quad B_{1,1} = 1.3894 \quad (tesla) \\ \frac{B_{1,1}(\lambda_2)}{B_{2d}} = 1.0518 \quad or \quad B_{1,1} = 2.5858 \quad (tesla) \end{aligned}$$

We comment here that the field components as described by Eq. (26) differs from the corresponding expression written in the Appendix of a paper by J.Blewett et al^d due to possible typographical errors in that paper. We also note that if we express the total current written in equation (31) in a form similar to that expressed in Blewett's paper we arrive at the total current per pole ($= 2I_0$)

$$Current/pole = \frac{5B_{1,1}\lambda_0}{\pi^2\left(\frac{\pi R}{L}K_0 + K_1\right)} \quad (39)$$

where $\lambda_0=2L$ (period). Blewett's expression for the current differs by a factor of $\sqrt{1 + \left(\frac{L}{\pi R}\right)^2}$

$$Current/pole = \frac{5B_{1,1}\lambda_0\sqrt{1 + \left(\frac{L}{\pi R}\right)^2}}{\pi^2\left(\frac{\pi R}{L}K_0 + K_1\right)} \quad (40)$$

For the case of a single pair of current carrying wires wound in a bifilar helix^e this expression is also different from both cases.

$$Current/pole = \frac{5B_{1,1}\lambda_0}{4\pi\left(\frac{\pi R}{L}K_0 + K_1\right)} \quad (41)$$

^d Orbits and fields in the helical wiggler — Journal of Applied Physics, Vol. 48, No. 7, July 1977

^e Static and Dynamic Electricity — W.R.Smythe, p.277.

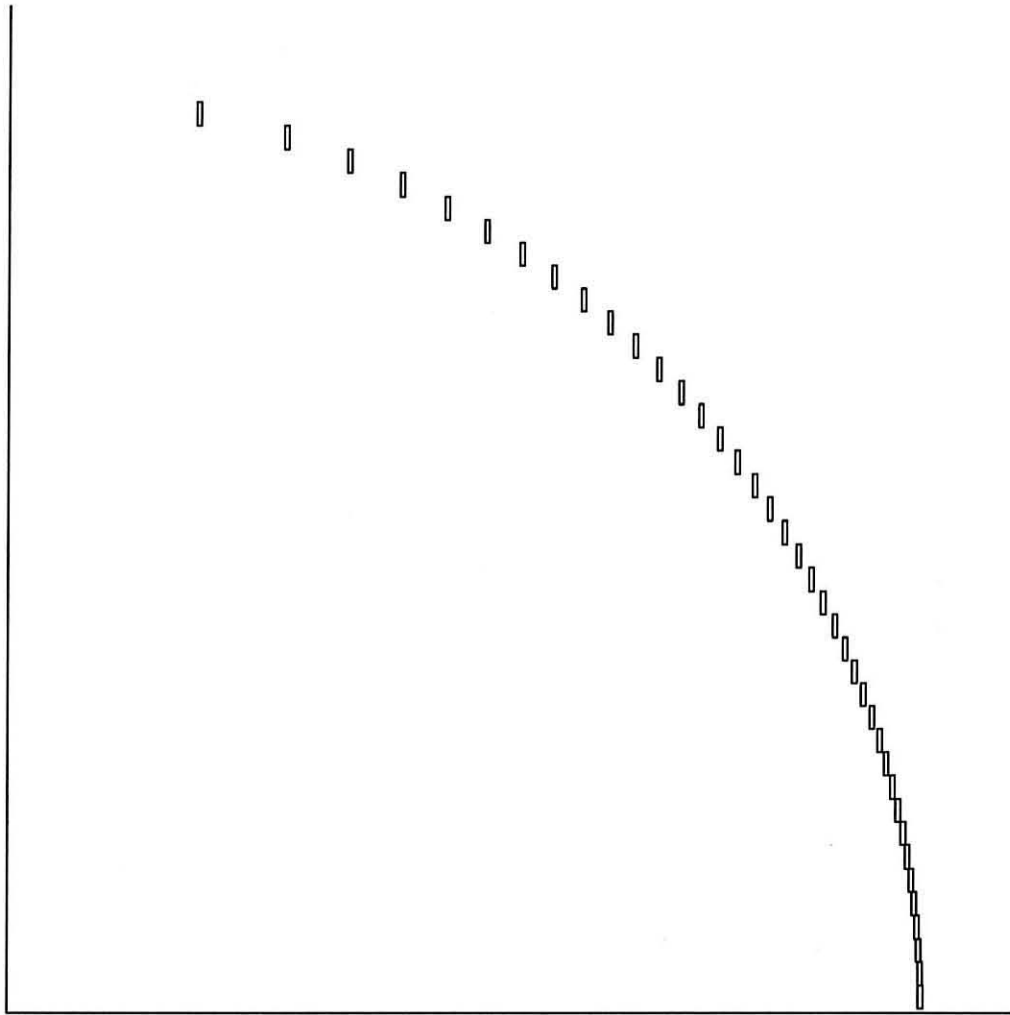


Figure 2 Winding cross section in a $\cos\theta$ configuration.

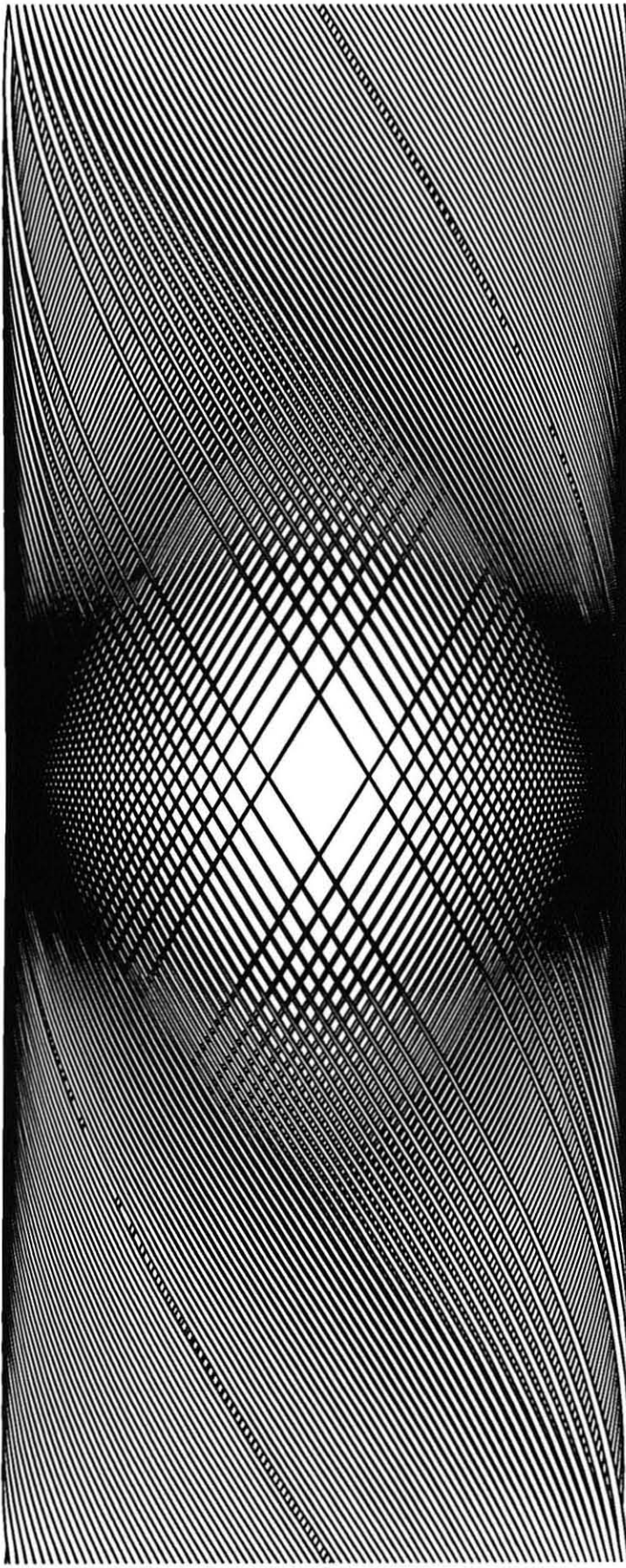


Figure 3 3D windings for half period $L=10$ in a $\cos(\pi z/L)$ configuration.

Appendix A Iron contribution

Equation (22) suggest a field enhancement factor arising from an iron sheet placed at $r=a$. Figure 4 shows such a factor for $n=1$ and $m=1$ as a function of $s = \frac{\pi R}{L}$ with the ratio of a/R used as a parameter.^f

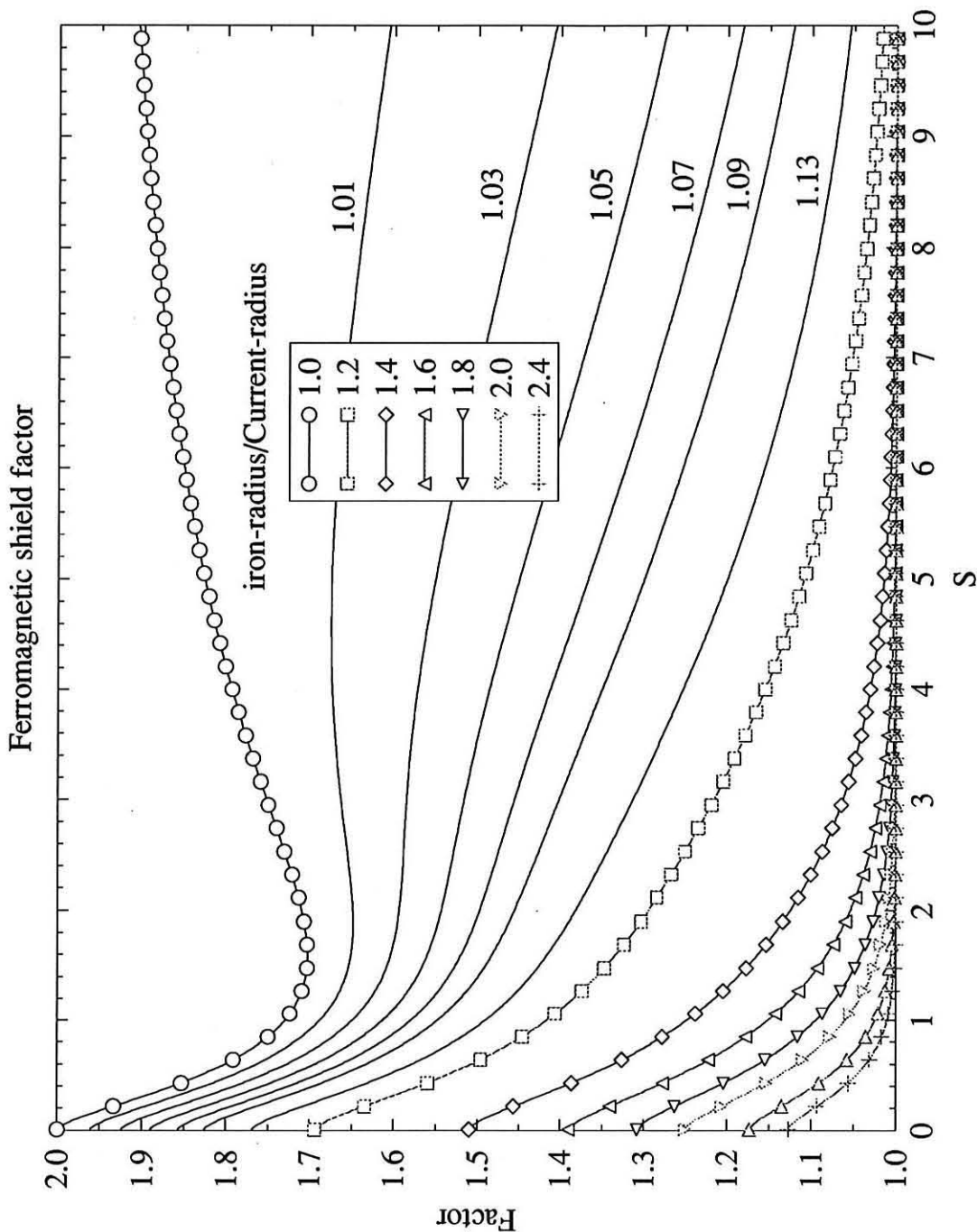


Figure 4 Field compression factor in a helical dipole wiggler.

^f I would like to acknowledge the help I received from Domenico Dell'orco in producing this graph.

Appendix B 3D harmonic coefficients

In order that the series for the potential V_n satisfy the differential equation (Eq. 1) we introduce the functions $A_n(z)$ and express the coefficients g_{rn} , $g_{\theta n}$, g_{zn} as general functions of r and z as shown below :

$$\begin{aligned} g_{rn}(r, z) &= \sum_{k=0} (-1)^{k+1} \frac{n!(n+2k)}{2^{2k} k!(n+k)!} A_n^{(2k)}(z) r^{2k} \\ g_{\theta n}(r, z) &= \sum_{k=0} (-1)^{k+1} \frac{n!n}{2^{2k} k!(n+k)!} A_n^{(2k)}(z) r^{2k} \\ g_{zn}(r, z) &= \sum_{k=0} (-1)^{k+1} \frac{n!}{2^{2k} k!(n+k)!} A_n^{(2k+1)} r^{2k} \end{aligned} \quad (1)$$

Explicitly we can write the above as :

$$\begin{aligned} g_{rn}(r, z) &= -nA_n(z) + \frac{n+2}{4(n+1)} A_n''(z) r^2 - \frac{n+4}{32(n+1)(n+2)} A_n''''(z) r^4 \\ &\quad + \frac{n+6}{384(n+1)(n+2)(n+3)} A_n''''''(z) r^6 - \dots \\ g_{\theta n}(r, z) &= -nA_n(z) + \frac{n}{4(n+1)} A_n''(z) r^2 - \frac{n}{32(n+1)(n+2)} A_n''''(z) r^4 \\ &\quad + \frac{n}{384(n+1)(n+2)(n+3)} A_n''''''(z) r^6 - \dots \\ g_{zn}(r, z) &= -A_n'(z) + \frac{1}{4(n+1)} A_n'''(z) r^2 - \frac{1}{32(n+1)(n+2)} A_n''''(z) r^4 \dots \end{aligned} \quad (2)$$

For the expressions of the skew terms just replace g_{rn} , $g_{\theta n}$, g_{zn} with \tilde{g}_{rn} , $\tilde{g}_{\theta n}$, \tilde{g}_{zn} and $A_n(z)$ with $\tilde{A}_n(z)$

The representation specified above for 3-D magnetic fields, can be written in terms of functions $A_n(z)$ and $\tilde{A}_n(z)$ and their derivatives for the example used in the main part of the paper where $n=1$ and $m=1$, such that :

$$\begin{aligned} A_1^{(2k)} &= (-1)^k \left(\frac{\pi}{L}\right)^{2k} B_{1,1} \cos \frac{\pi z}{L} \\ \tilde{A}_1^{(2k)} &= (-1)^k \left(\frac{\pi}{L}\right)^{2k} B_{1,1} \sin \frac{\pi z}{L} \\ A_1^{(2k-1)} &= (-1)^k \left(\frac{\pi}{L}\right)^{2k-1} B_{1,1} \sin \frac{\pi z}{L} \\ \tilde{A}_1^{(2k-1)} &= (-1)^{k+1} \left(\frac{\pi}{L}\right)^{2k-1} B_{1,1} \cos \frac{\pi z}{L} \end{aligned} \quad (3)$$

In the next series of graphs we include results of such A's (both normal and skew) computed by the program "figends" for one of the example previously noted ($2L=5.0$). We note the sinusoidal periodicity of the A's and their derivatives according to the above relations.

Helical wiggler 2L=5.0 - Normal

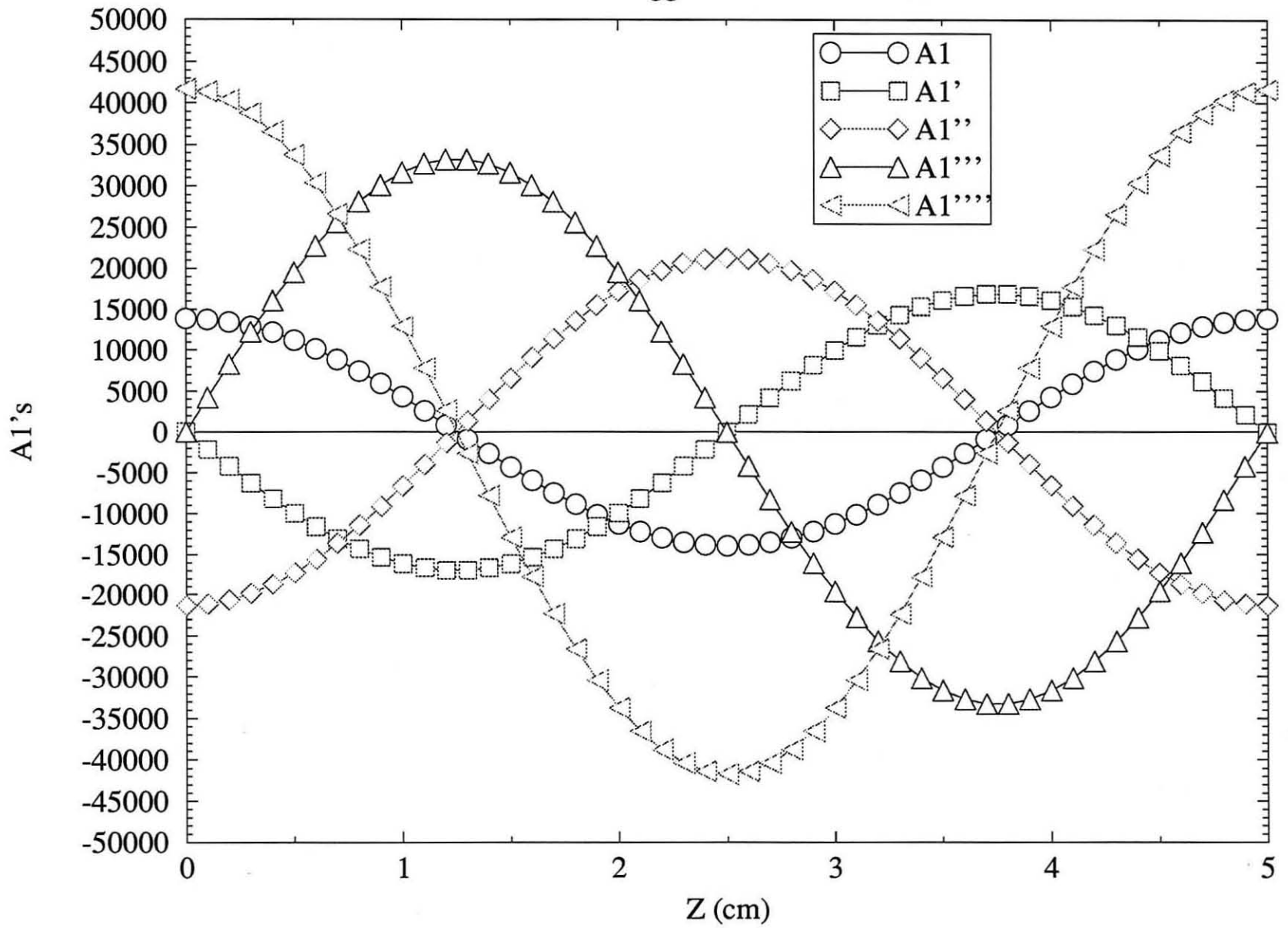


Figure 6 Normal A_1 as a function of z over a full period..

Helical wiggler 2L=5.0 - Normal

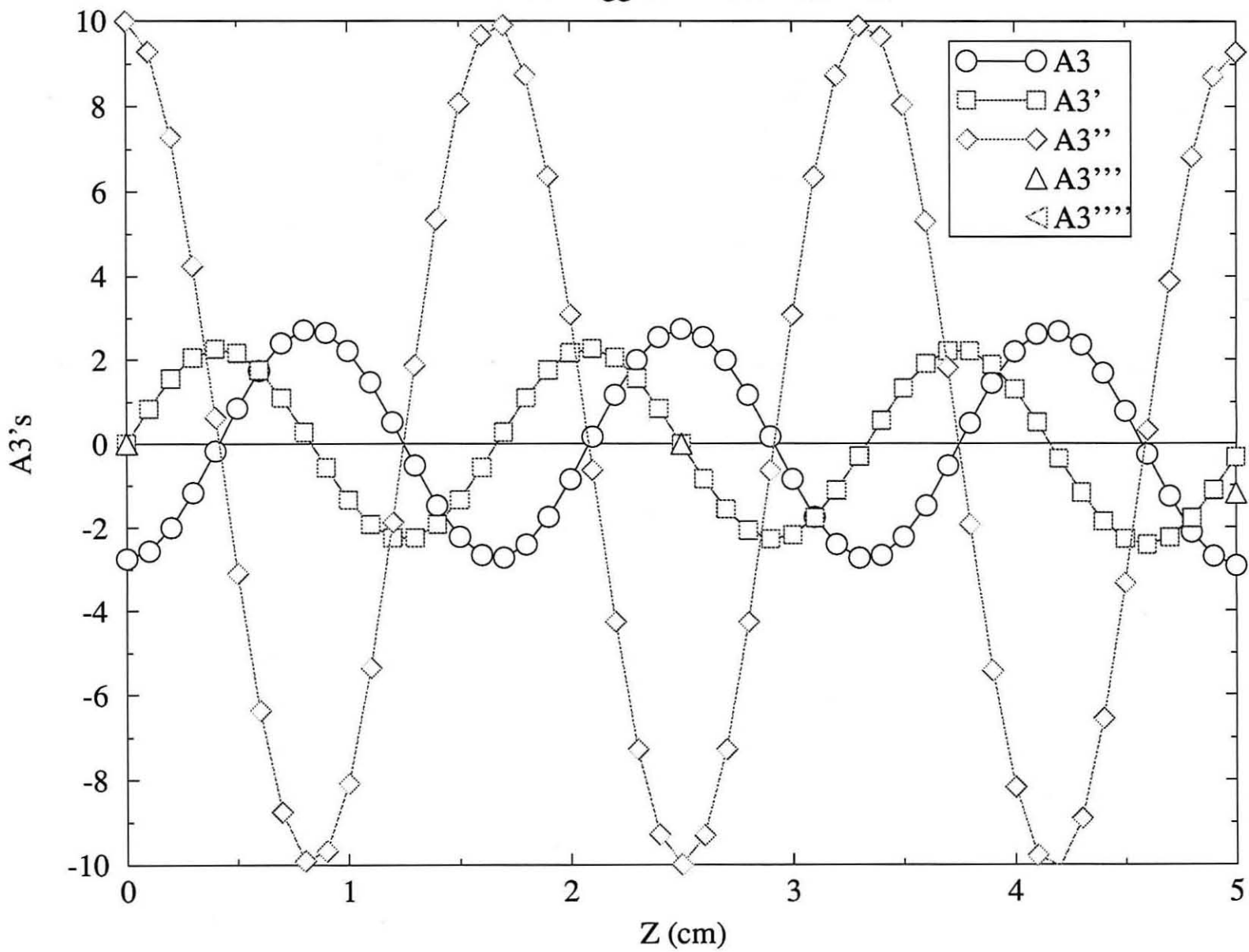


Figure 7 Normal A_3 as a function of z over a full period..

Helical wiggler 2L=5.0 - Normal

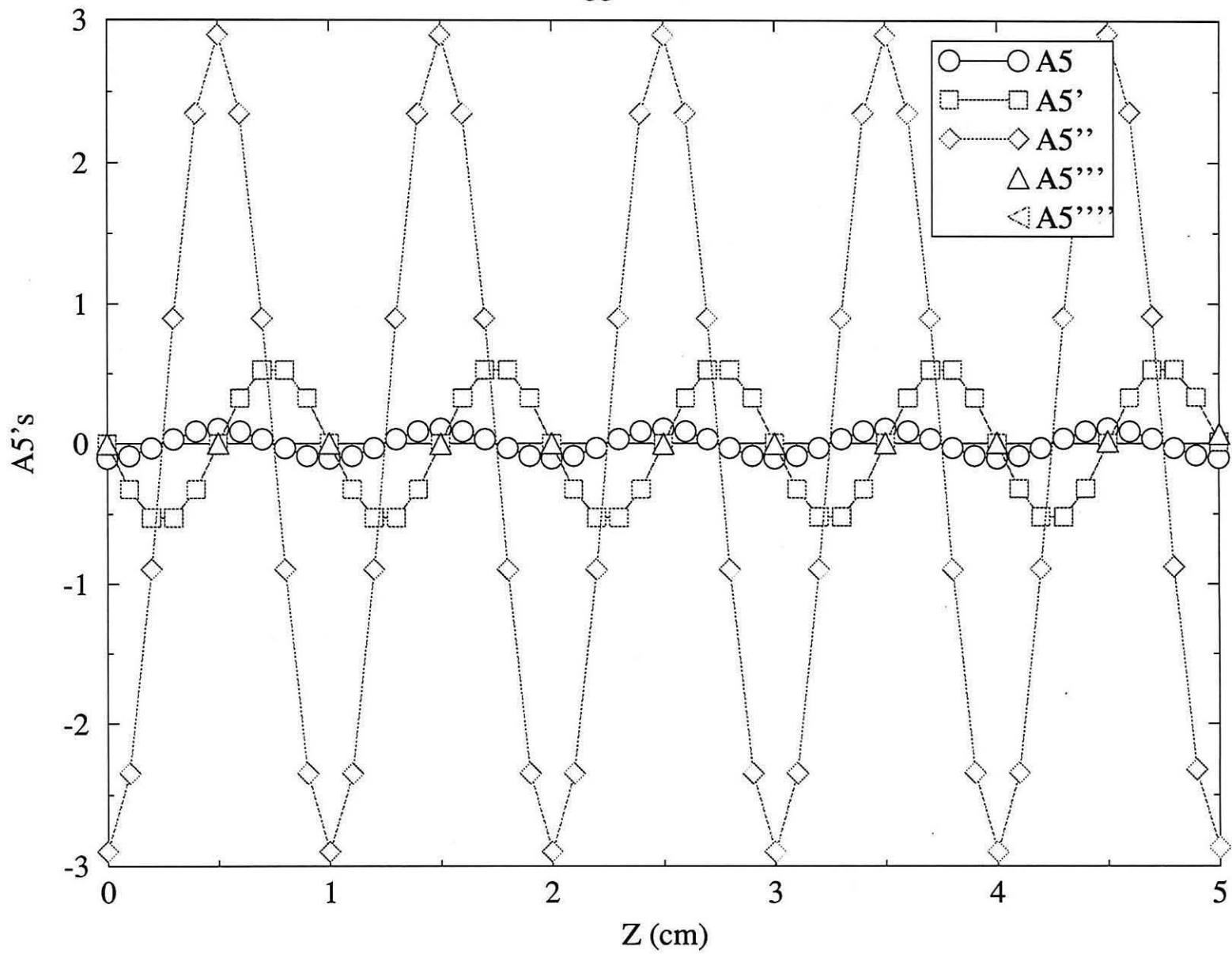


Figure 8 Normal A5 as a function of z over a full period..

Helical wiggler 2L=5.0 - Normal

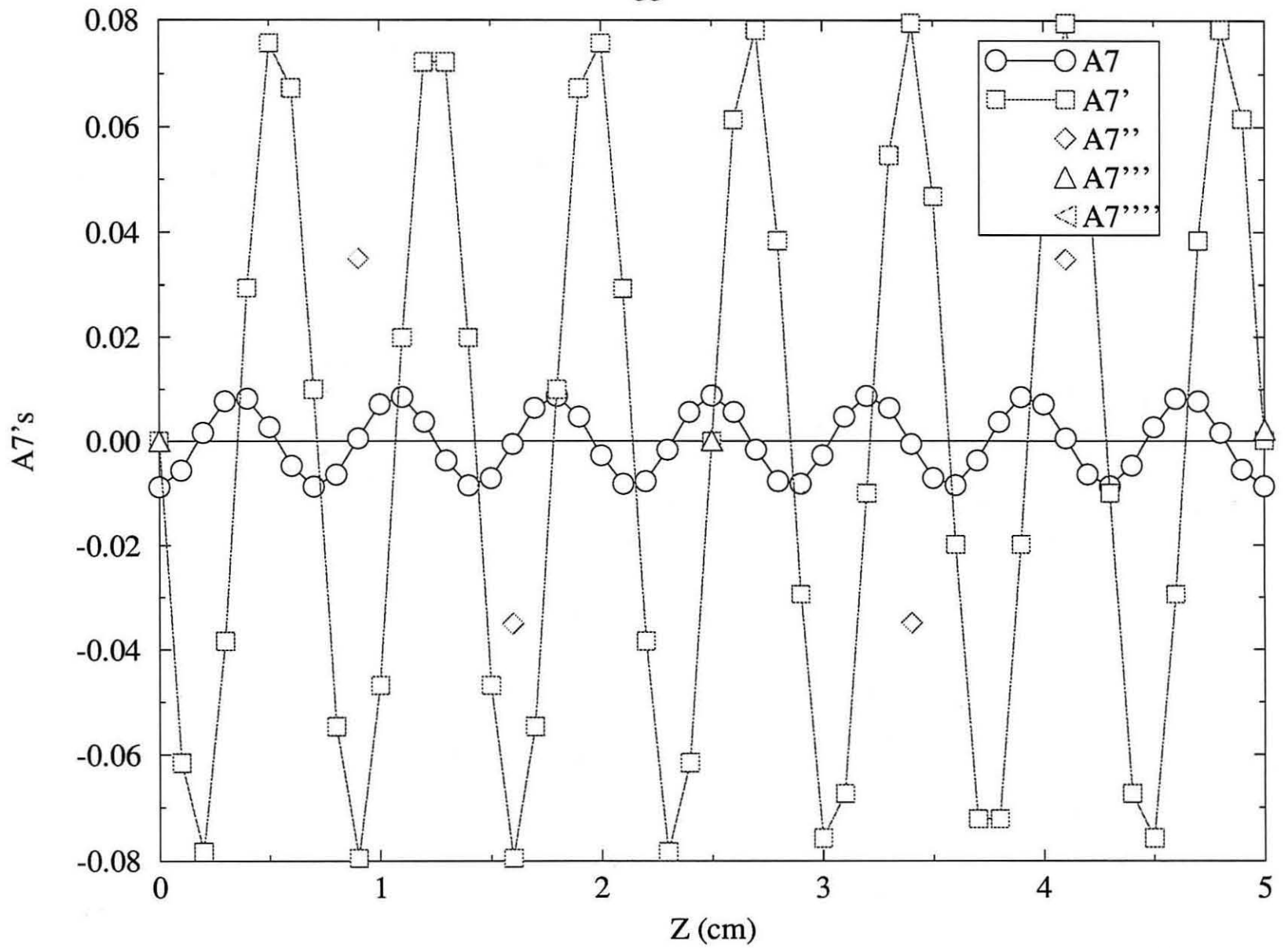


Figure 9 Normal $A7$ as a function of z over a full period..

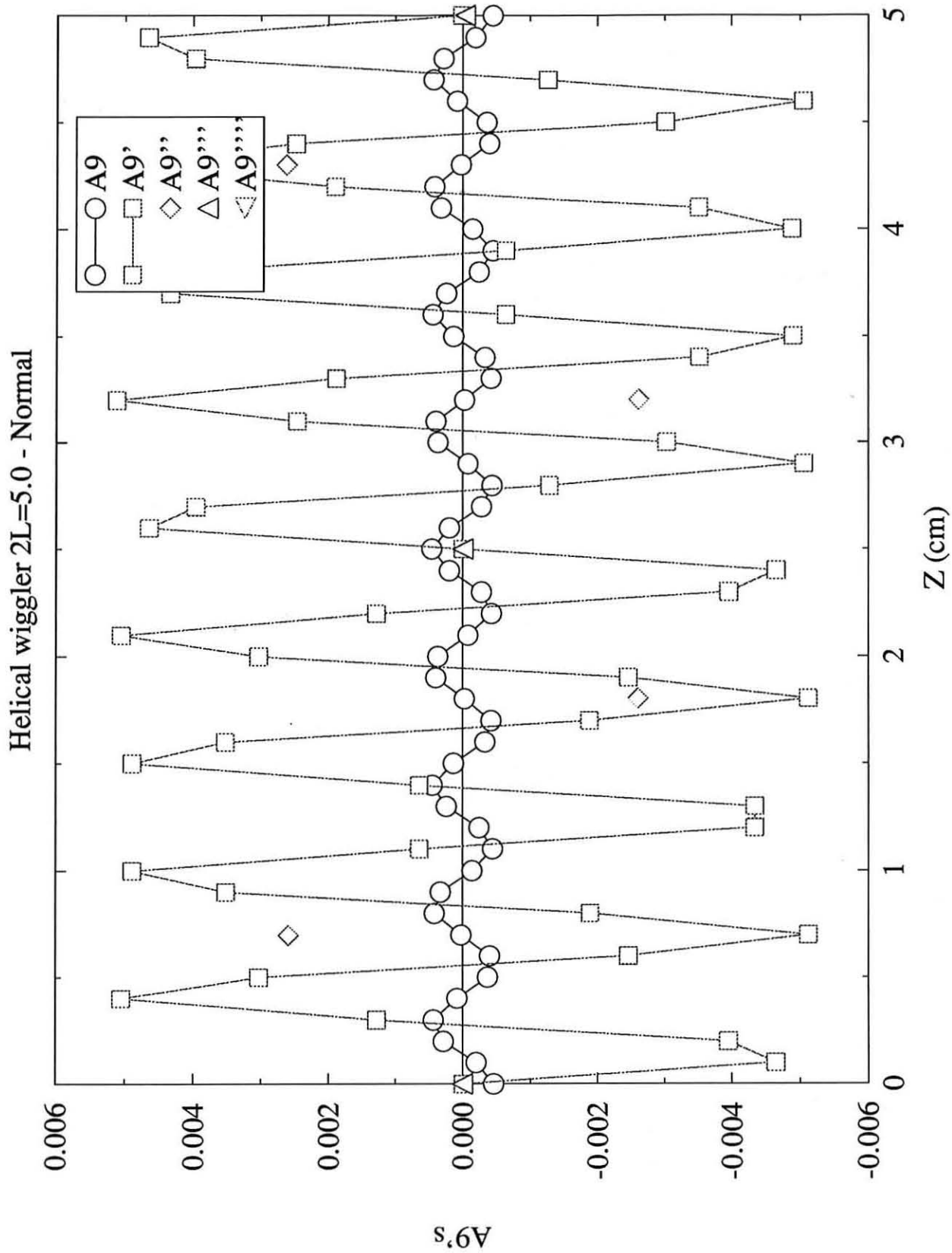


Figure 10 Normal A9 as a function of z over a full period..

Helical wiggler $2L=5.0$ - Skew

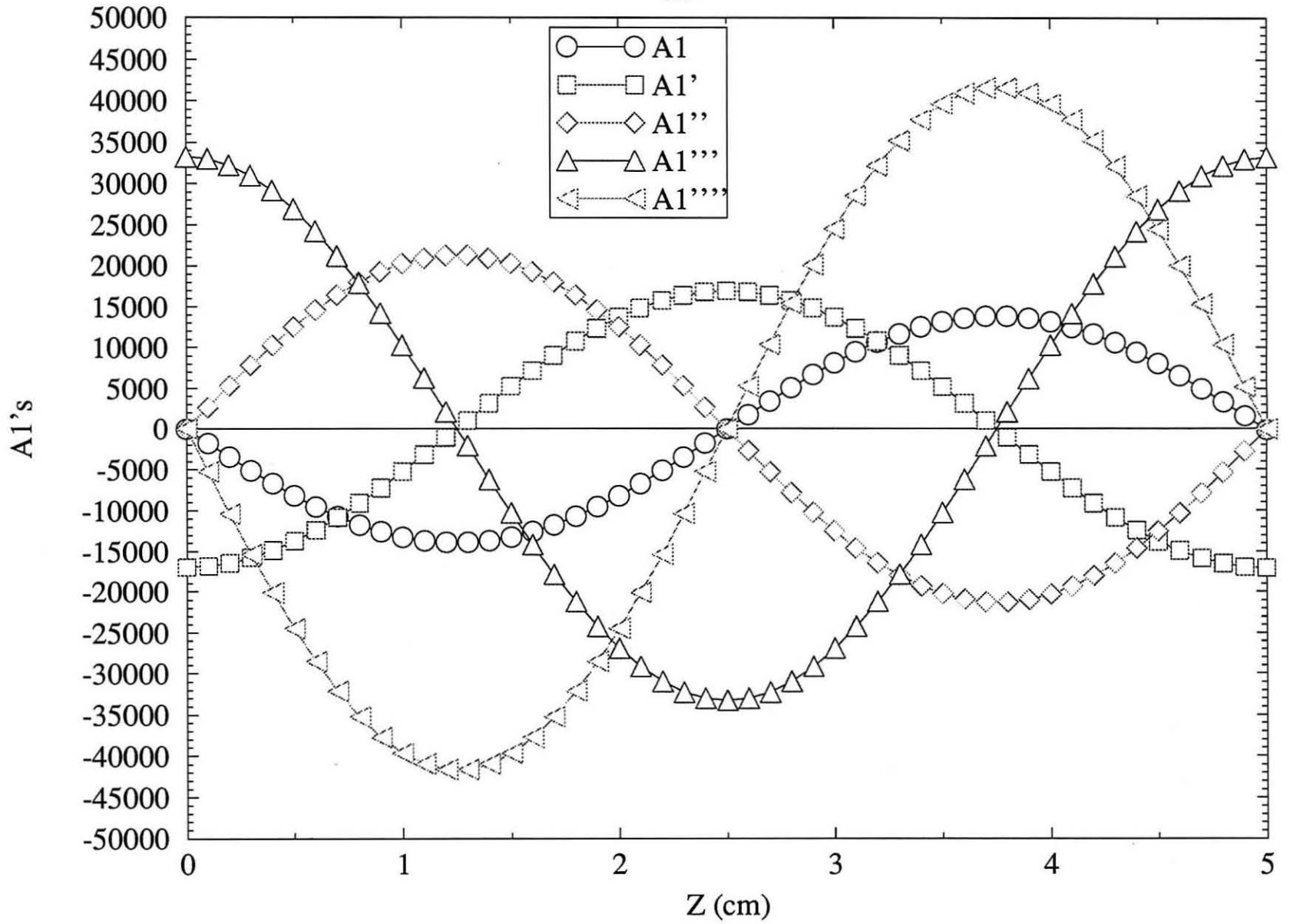


Figure 11 Skew $A1$ as a function of z over a full period..

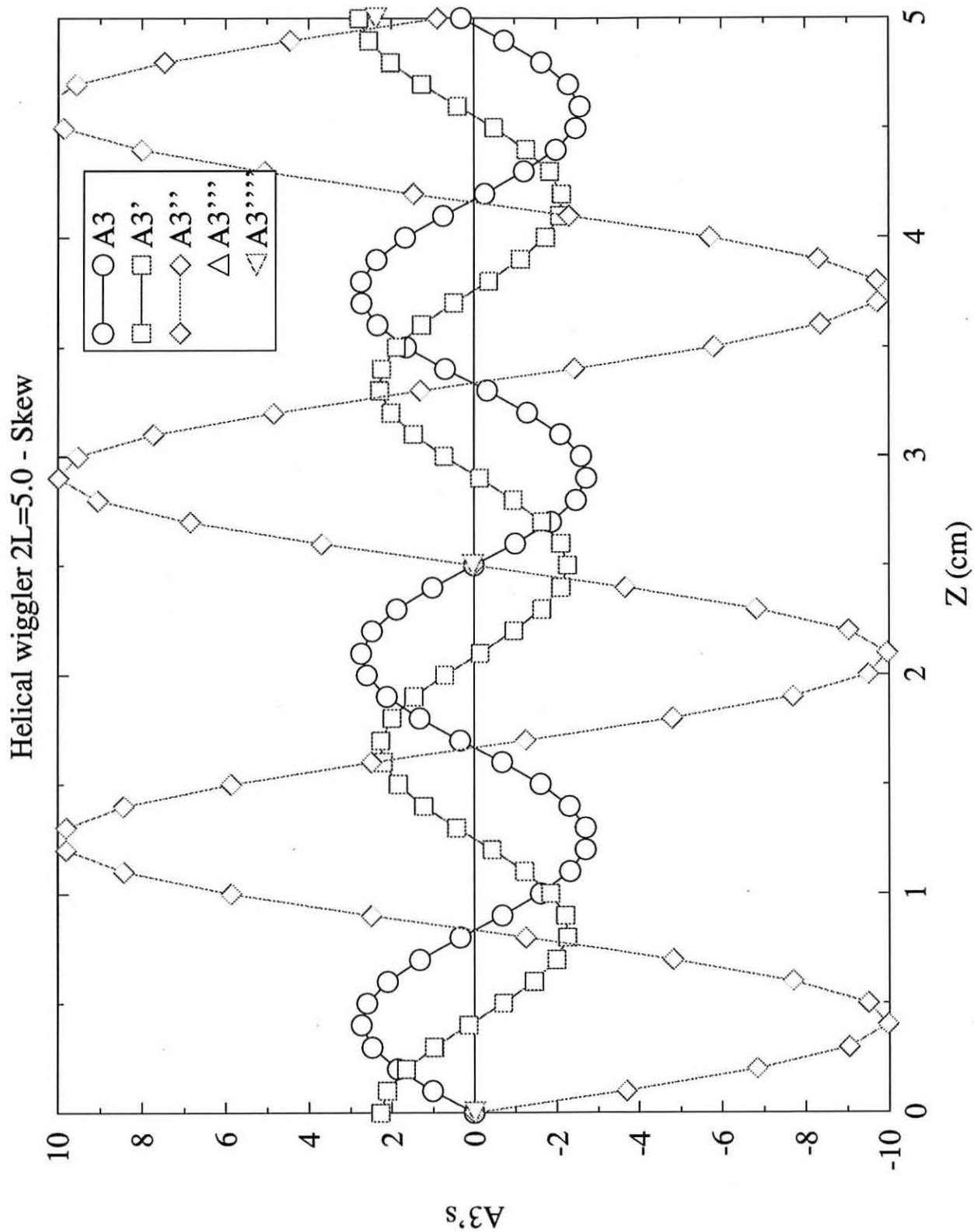


Figure 12 Skew A3 as a function of z over a full period..

Helical wiggler 2L=5.0 - Skew

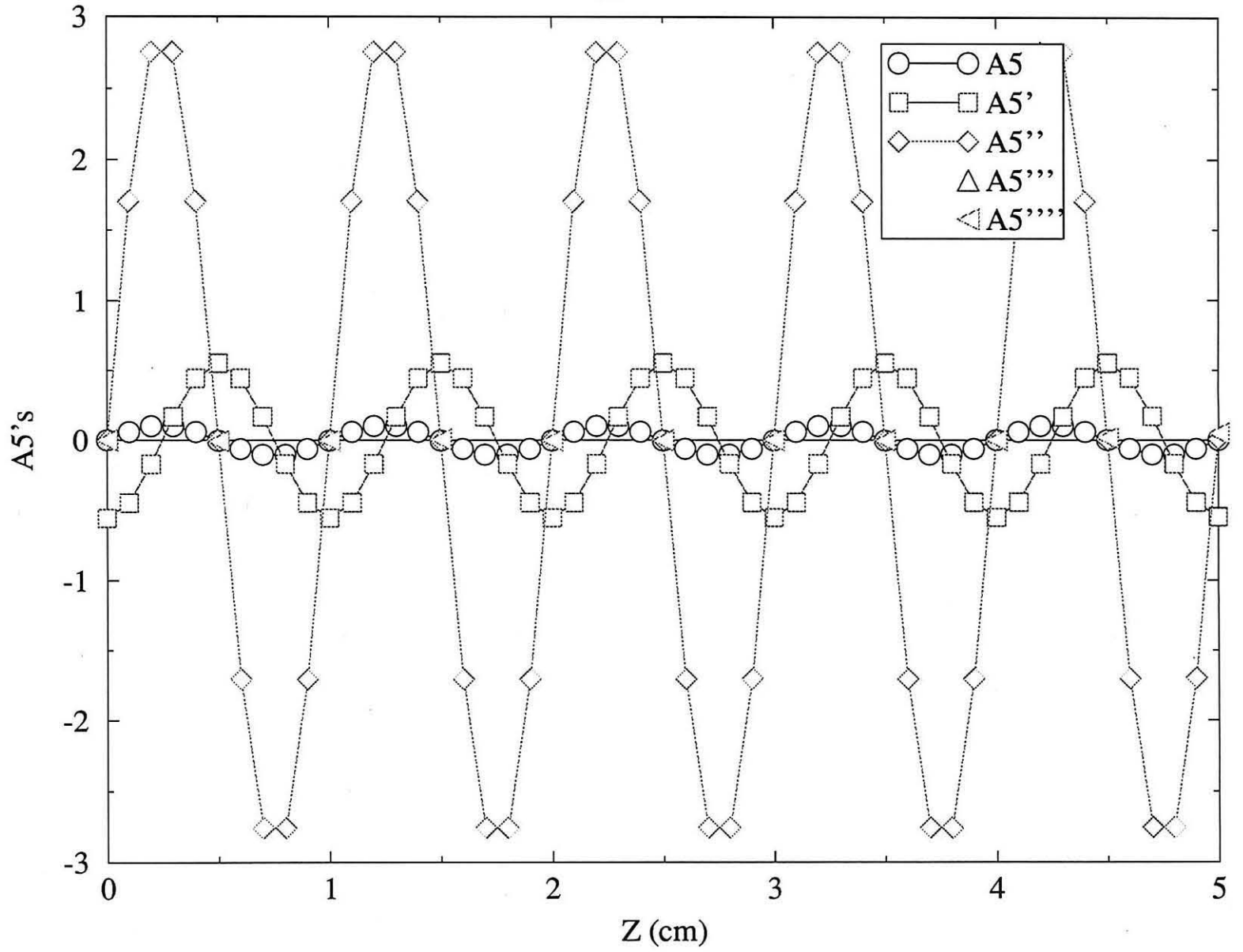


Figure 13 Skew $A5$ as a function of z over a full period..

Helical wiggler $2L=5.0$ - Skew

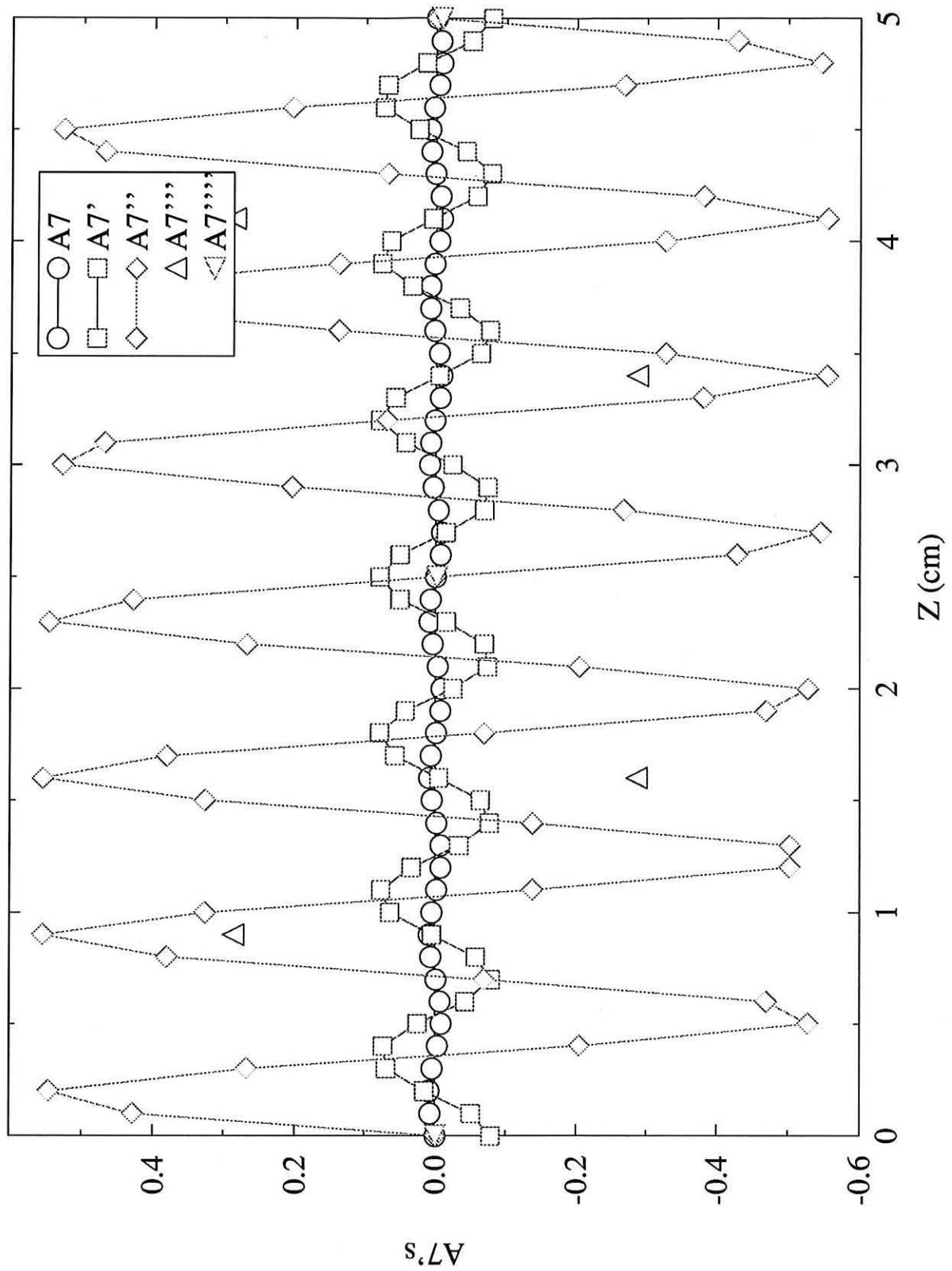


Figure 14 Skew $A7$ as a function of z over a full period..

Helical wiggler 2L=5.0 - Skew

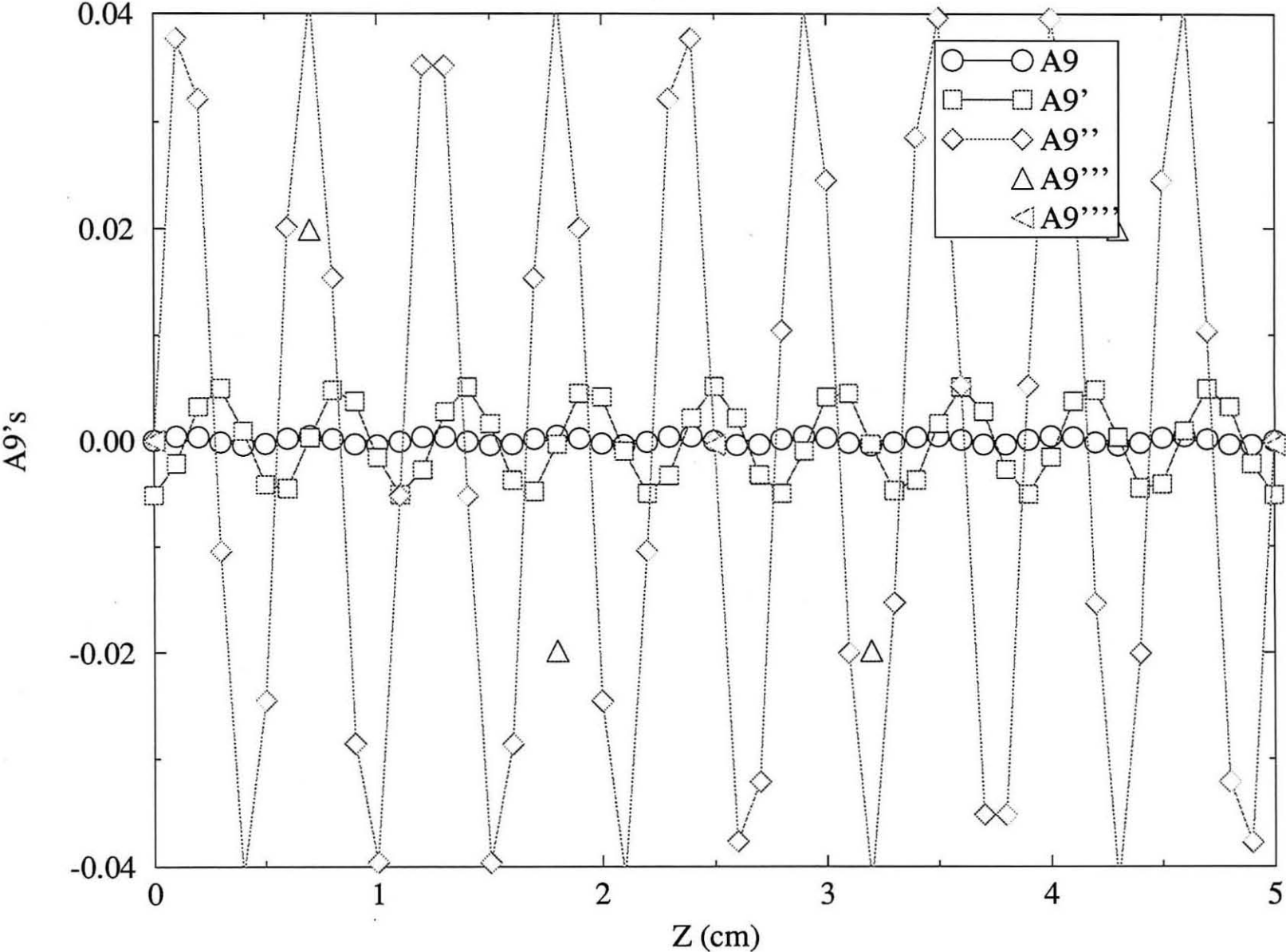


Figure 15 Skew A9 as a function of z over a full period..